Taylor & Francis
Taylor & Francis Group

AVIATION
ISSN 1648-7788 / eISSN 1822-4180
2017 Volume 21(1): 9–16
doi:10.3846/16487788.2016.1264720

RESEARCH OF THE MICROMECHANICS OF COMPOSITE MATERIALS WITH POLYMER MATRIX FAILURE UNDER STATIC LOADING USING THE ACOUSTIC EMISSION METHOD

Aleksandrs URBAHS[1], Muharbijs BANOVS[2], Kristine CARJOVA[3], Vladislavs TURKO[4], Jurijs FESHCHUK[5]

Institute of Aeronautics, Riga Technical University, Kalku str. 1A, k-1, LV-1658 Riga, Latvia
E-mails: [1]aleksandrs.urbahs@rtu.lv; [2]muharbijs.banovs@rtu.lv; [3]kristine.carjova@rtu.lv (corresponding author); [4]vladislav.turko@rtu.lv; [5]ndt_ae@mail.ru

Received 27 August 2015; accepted 17 November 2016

Aleksandrs URBAHS *graduated from the Faculty of Mechanical Engineering, Riga Civil Aviation Engineering Institute in 1981. In 1986 he was awarded a Dr sc.ing. degree by the same faculty. In 1997 he was awarded a Dr.habil.sc.ing. degree by Riga Aviation University. In the period from 1989 to 1999 – Vice Dean and Dean of the Faculty of Mechanical Engineering, Riga Aviation University. Since 1999 – full-time Professor at Riga Technical University. In the period from 1999 to 2012 – Head of the Institute of Transport Vehicle Technologies at Riga Technical University. Since 2012 – Head of the Institute of Aeronautics at Riga Technical University. He holds more than 20 patents and has published more than 320 scientific papers.*
His fields of research: aeronautics, nanomaterials, non-destructive testing, structural materials, unmanned vehicles, transport systems and logistics.

Muharbijs BANOVS *graduated from Riga Civil Aviation Engineering Institute as a Mechanical Engineer of Aircraft and Engine Maintenance in 1975. In 1979 he was awarded a Doctoral Degree, Faculty of Aircraft Repair and Technology, Riga Civil Aviation Engineering Institute. 1981–1995 – Assistant, Assistant Professor, Professor, Lecturer of Riga Civil Aviation Engineering Institute. 1995–1998 – Assistant, Assistant Professor, Professor, Lecturer of Riga Aviation University. Since 1999 – Assistant, Assistant Professor, Professor, Lecturer of Riga Technical University of Institute of Transport Vehicle Technologies. Since 2007 he has been conducting Supreme State Engineering Courses of Improvement of Qualification on Non-destructive Testing.*
His fields of research: aeronautics, non-destructive testing.

Kristine CARJOVA *graduated from the Faculty of Mechanical Engineering, Transport and Aeronautics, Riga Technical University in 2016 and received a Dr sc. ing. degree. In 2010 she obtained a degree of Master of Science at the Latvian Maritime Academy. She graduated from Latvian Maritime Academy and obtained a Specialisation of Engineer–Ship Navigator. Work experience: 2004 to 2007 – Navigator of Merchant Vessel. 2009 to 2011 – Captain on ASD tugboat at JSC PKL Flote. Since August 2011 – Researcher at the Institute of Aeronautics, Riga Technical University.*
Her fields of research: aeronautics, non-destructive testing, structural materials, unmanned vehicles.

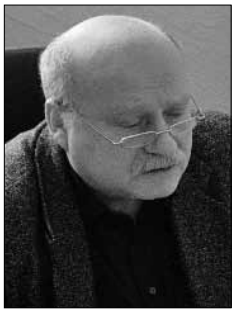

Vladislav TURKO *received a Doctoral Degree from the Aviation Institute, Riga Technical University in 2013. 1979 – 1982 – Postgraduate studies, Faculty of Aircraft Repair and Technology, Riga Institute of Civil Aviation Engineers named Lenin Komsomol. 1968 – 1974 – Mechanical Engineer of Aircraft and Engine Maintenance, Riga Institute of Civil Aviation Engineers named Lenin Komsomol.*
Work experience: since 2013 – Deputy Director (scientific issues). 2009–2013 – Deputy Director (ISO quality system). 1997–2009 – Technical Director, Riga scientific and experimental centre "Aviatest LNK" Ltd. 1992–1997 – Senior Scientist at RSEC "Aviatest LNK" Ltd., Scientist at Riga branch GosNII GA.
His fields of research: material fatigue, fatigue cracks, acoustic emission, ultimate loads and strain, fatigue mathematical models.

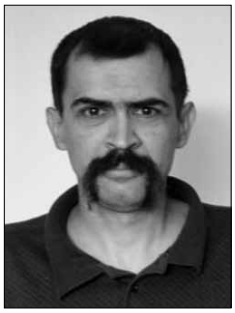

Jurijs FESHCHUK *has been a Doctoral Student at the Institute of Aeronautics, Riga Technical University since 2012. He has been awarded MSc eng in 2016 at the Institute of Aeronautics, Riga Technical University.*
His fields of research: material fatigue, fatigue cracks, acoustic emission, ultimate loads and strain, fatigue mathematical models.

Abstract. Micromechanics of composite materials' failure has been investigated under static loading by means of acoustic emission (AE) method. The results showed that for samples made of fiberglass with transverse fibers with respect to the applied load, the process of destruction both in the deformation parameters and in the parameters of total AE has two stages of damage accumulation. At the same time the parameter of total AE shows that the process of destruction begins 5–6% earlier than it is shown by the deformation parameter. Also the nature of the total AE change was analysed.

Keywords: composite materials, polymer matrix, static loading, acoustic emission, micromechanics.

1. Introduction

Composite materials (composites) are designed to improve such mechanical characteristics as strength, specific strength, hardness, specific viscosity and heat resistance. A composite consists of a base (or matrix) distributed with certain regularity in the form of a fiber reinforcer or as dispersed particles.

There are composite materials with two types of matrix: with a metallic or a polymer base. Both of them are becoming increasingly widely used in automobile industry, for aircraft airframes, engines, etc., as they have a range of physical and chemical properties that cannot be obtained by using conventional alloys. For example, metal-based composites reinforced with ceramic fibers have a high heat resistance, a relatively low specific gravity and in comparison to conventional alloys have a higher fatigue strength. Their temperature capability (the ratio of the temperature at which the tensile strength is 14 kgf/mm^2 to the melting temperature) is 0.80–0.98. Polymer based composites reinforced with carbon fibers have a low density (up to 3 g/cm^3), a high modulus of elasticity (15 000–20 000 kgf/mm^2) and a low linear expansion coefficient (2–5 * 10^{-6} °C $^{-1}$) as well as a relatively low price. They have a high specific rigidity and strength in the direction of reinforcing. This combination of properties is unachievable in conventional alloys because light metals (aluminium, magnesium) with a density of 1–7 g/cm^3 have a modulus of elasticity of 5000–7000 kgf/mm^2 and a very high linear expansion coefficient (20–25 * 10^{-6} °C $^{-1}$) (Pridancev 1978). In fibrous composites the main purpose of the fibers is to carry the load while the matrix passes the load and distributes it between them. Consequently, the mechanical properties of the composite depend primarily on the properties of the fiber and the matrix. The transfer of stress from the matrix to the fiber occurs across the interface between them, and the question of nature of the bond in the fiber-matrix interface is one of the most important and least studied. Furthermore, the strength of fibrous compositions depends on the volume content of fibers in them and varies linearly with the concentration of fibers from 5% to 80%. It is not possible to impregnate and moisten all fibers with the matrix if the concentration exceeds 80%. It impairs the ability of the matrix to transfer stress and fully convey the stress to the fibers. Eventually, the condition of the fiber-matrix interface and the nature of the fiber-matrix interconnection determine the strength and load capacity of the entire composition. The optimal behavior of the composite, in its turn, depends on the "structural unity" of its components, which assumes good interconnection among all the elements of the

reinforcement and the matrix providing a uniform transmission of forces from component to component along with their structural deformation as one piece.

Compositions providing the above described structural unity are considered to be perfect or "model", for example, compositions with parallel fibers that stretch along the fiber (Korten 1970). In this case, the aim of the research is to reveal the nature of destruction and to theoretically evaluate the tensile strength of a "model" of the composition, as well as to find the answer to the question of what caused the damage of the structural integrity, which may be conditioned by the presence of cracks formed together during the manufacturing process or under the influence of stress and environment in the process of loading. For example, compositions made of strong plastic fibers and a plastic matrix, which adhere well to each other, are usually destroyed because of plastic flow instability. In another case, the strength of a composition depends on the combination of tensile strength fibers and the matrix, as well as the matrix tensile strength in shear. In both cases, the strength of the fibers and the matrix is quantitatively reproduced and determined on the basis of the plastic properties of both materials. At the same time, the strength of each of them has a minimum variation. Therefore, the strength of such a "model" composition can be expressed by the mean strength of the fibers, the matrix and the volumetric content of the composition components. The analysis of the properties of these compositions assumes the simplest possible consideration of the effect of several important parameters, i.e. the volume fraction of long fibers and the ratio of fiber length to the diameter of fibers of finite length.

Such an analysis serves as a convenient starting point describing the behavior of the composition based on the average fiber strength, the essence of which is to analyze the behavior of the composition tensile strength and the fracture "model" compositions reinforced with fibers with the same strength. Therefore, in McDanels *et al.* (1963) and Kelly *et al.* (1965) it is proposed to divide the "Stress-Strain" curve during the static loading into several stages of destruction for different compositions. For example, according to McDanels *et al.* (1963), for compositions with a fiber volumetric fraction of 0.25, 0.50 and 0.75 made up of plastic filaments (Fig. 1 – dashed line) and the plastic matrix (Fig. 1 – solid lines) the curve is divided into the following four stages: 1) elastic deformation of the fibers and matrix; 2) elastic deformation of the fibers and plastic deformation of the matrix; 3) plastic deformation of the fibers and the matrix; 4) further plastic deformation accompanied by the appearance of discontinuous fibers which, when accumulated, lead to the destruction of the composition. All four stages show up if the matrix and the fibers are plastically deformed. If the fibers are brittle (Fig. 1), Stage 3 is not present and Stage 4 may be very short.

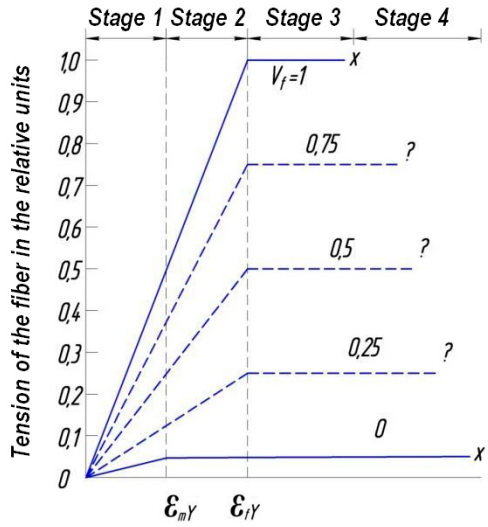

Fig. 1. Stress-strain diagram of a "model" composition (dashed lines) consisting of plastic filaments and a plastic matrix (solid lines): V_f – volumetric fraction of fibers, ε_m and ε_f – the proportional limit of the matrix and fibers (McDanels *et al.* 1963)

On the other hand, the behavior of compositions based on a plastic matrix reinforced with strong brittle fibers of finite length is more complicated. In this case, there are at least two types of failure: either due to the occurrence of the first rupture or due to multiple fibers of finite length being torn. In the first case, the fracture cross-section coincides with the fiber fracture cross-section, which lets us suggest that, after the destruction of the first fiber, the remaining fibers are overloaded. Moreover, the elongation of the composition is comparable to the fragile fiber elongation. The second type of failure is the evidence of either a weak adhesion between the fibers and the matrix, insufficient strength of the matrix, or of the defects generated during fabrication. When calculating the tensile strength of such compositions both types of fracture must be taken into account.

The behavior of the composition is quite complicated if it includes a combination of fragile fibers (e.g., fiberglass) with a large variation of tensile strength and a semi-brittle matrix (for example, epoxy resin). The process of destruction in this case occurs due to the accumulation of a critical number of fiber breaks, which eventually extend in parallel to the fibers by crack propagation either in the matrix or on the surface of the section perpendicular to the fibers, which results in the degradation forming very ragged edges. Strength theories on such compositions use a statistical fiber strength characteristic and a certain criterion for the critical accumulation of fiber breaks, which is based on the analysis of the beam strength; a connection is established between the statistical nature of the fiber strength and the strength of the composition in general. This problem was considered for the first time by Parratt (1960), who suggested that the destruction of

the composition occurs at the moment when the growing destruction of fibers leads to the shear failure of the matrix, and a further increment of load cannot be transferred to other fibers, because the shear strength limit of the matrix has been reached.

The above discussed composition models do not give an exhaustive answer to the question of the ultimate strength and nature of destruction due to the composition tension. These models roughly simplify the real material and are only intended to qualitatively describe the phenomenon. Experimental methods used to study the mechanics of composites, such as the method of photoelasticity, the strain method, the moire and holography, for example, (Deniel 1978), do not solve the problems associated with the destruction at the micro level. Therefore, it is clear that we need further experimental research in order to reveal the actual mechanisms of the deformation and destruction and take them into account in the theoretical models aimed at determining the strength of composites. For this purpose, we used the method of acoustic emission (AE) characterized by a high sensitivity to destruction mechanisms at the micro level (Urbach *et al.* 2011).

2. Samples and test procedure

Tensile tests were carried out on two groups of samples made of fiberglass (Fig. 2) with both warp and weft fibers, which can be regarded as a structural feature. The first group includes samples with transverse warp fibers relative to the applied force (Fig. 2a), the second sample is the same, however it has longitudinally orientated base fibers relative to the same applied force (Fig. 2b). The second group containing samples made of fiberglass also included samples made of the CFRP. A sample (Fig. 2) is a plate of a rectangular shape (2) fixed on the upper and lower ends of plates 1 and 6 under the testing machine clamps. The tension and acoustic emission sensors were attached beforehand.

Figure 3 shows a measurement system of the switching circuit used for these tests. For the reliability and validity of the AE research two different devices connected to the same AE sensor 2 were used: the AE unit 10 (AF-15, Moldova) is the receiver of AE signals with a bandwidth of 20 kHz – 2.0 MHz and the AE unit 9 (POCKET AE-2, USA) allows fixing the parameters of AE signals in a frequency band from 1.0 kHz to 1.0 MHz. For a preliminary amplificatin of the AE signals, for the device AF-15, preamplifier 8 with a 40 dB amplification in the frequency range from 20 kHz to 2 MHz was used, while for the device POCKET AE-2, preamplifier 7 with a 26 dB amplification in the frequency range from 100 kHz to 1 MHz was used. During the loading of the samples, the device AF-15 fixed the total AE, while the device POCKET AE-2 fixed the values of the total AE, amplitude, intensity, energy and the duration of AE signals.

The task of obtaining the AE signal change dependence directly during the process of loading with the help of the AF-15 device was solved by using a data acquisition card (11) (Fig. 3). In addition to the AE data, this card received the data from the strain gauge module's (12) tension sensors (3), which contained the information about the load power, the amount of piston movement and the deformation. A similar problem in the device POCKET AE-2 was solved using its parametric input, which received the load data from the dynamometer (6) (Fig. 3) of the loading system (5).

To prevent the reception of false AE signals from the locations where the samples are clamped in the clamps (4) (Fig. 3) of the traverse testing machine, the testing technique assumed a preliminary compression of each sample in the places where the upper and lower pads (6) are fixed (Fig. 2) of a force of one and a half times the work force in the jaws at which the sample is statically loaded. In this case, in these places it is possible to observe the Kaiser Effect (known in AE) which allows

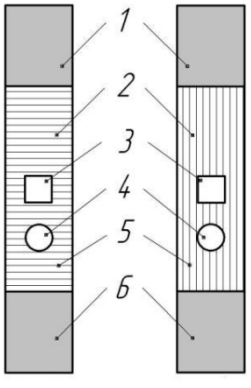

a) b)

Fig. 2. Sample and scheme

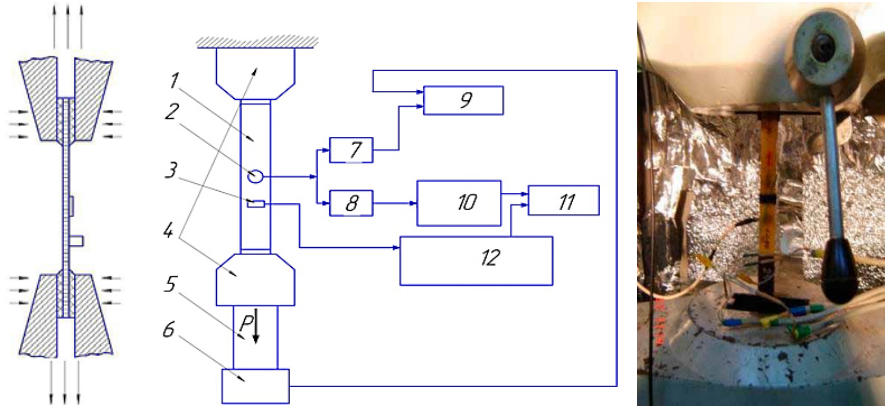

a) b) c)

Fig. 3. Measuring the complex switching diagram (a), the sample clamping diagram (b) and the sample in clamps (c): 1 – Sample; 2 – AE sensor; 3 – tension sensor; 4 – clamp; 5 – loading system; 6 – dynamometer; 7 and 8 – preamps; 9 – AE device POCKET AE- 2 (U.S.); 10 – AE-15 unit AF (Moldova); 11 – card data collection; 12 – strain module

obtaining the entire information solely from the AE zone between the clamps which is subject to destruction in the process of static loading.

3. Test results of fiberglass samples

For ease of analysis and comparative evaluation of the test data, the graphs are presented in relative units. Some results of these studies devoted to the experimental studies of the fracture mechanics of composites under tension using AE are shown in (Urbahs *et al.* 2012, 2011). In this article, the analysis of the results is continued by introducing the concept of the stages of damage accumulation. Moreover, an attempt to recognize the subtle phenomena of the nature of the fiberglass destruction was made by using electron microscopy. For example, when testing the samples with transverse based fibers relatively to the tensile strength (Fig. 4), a two-stage nature of the composite deformation in both the deformation parameters (areas 1 and 2) and in the summary parameters of AE (portions 11 and 21) was revealed: the stage of proportional changes in these parameters due to stress (sections 1 and 11) and the stage of intensive increment characterizing the beginning of the process of irreversible destruction of the composite (sections 2 and 21).

Curves in both the deformation parameter and the AE parameters are similar to the AE curve characterizing the deformation behavior of a pure matrix (see Fig. 1, curve $V_f = 0$), i.e. the matrix with a zero volumetric fraction of fibers and the absence of weft fibers having strongly elastic, as seen from the figure, the deformation stage and the stage of fluidity. In our case, the presence of weft fibers, along which the process of loading occurs, leads to the redistribution of the load, one part of which is felt by the weft fibers themselves and the other part falls on the matrix thus eliminating the stage of pure strength observed in Figure 1 (curve with $V_f = 0$). As seen from Figure 4, the process of permanent deformation (Stage 2 composite fracture) starts at about 0.8 of the breaking stress of the deformation parameter (border areas 1 and 2) and 0.75 of the failure stress of the total AE parameter (border areas 11 and 21). As in this

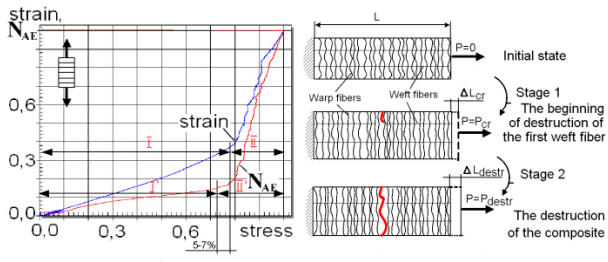

a) b)

Fig. 4. Curve of the total AE change and deformation due to the stress-strain and the assumed mechanism of destruction of the composite with a transverse warp fiber position relative to the tensile strength (B)

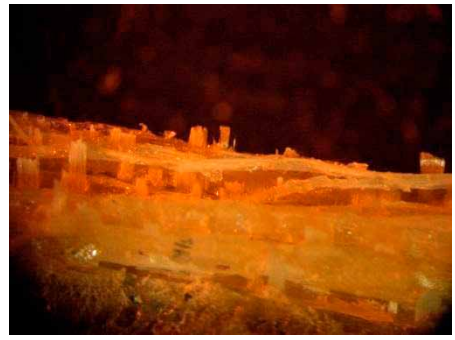

Fig. 5. A macro photo of a fragment of the destroyed sample portion (×30)

case the warp fibers have almost no load, this type of destruction is characteristic to the destruction of the matrix partially, i.e. epoxy resins, and partially of the weft fibers. Figure 5 shows a photograph of a fragment of one of the damaged sections of the composite whose curve is shown in Figure 4a. The photograph shows the destroyed weft fibers and the matrix.

The assumed mechanism of destruction of this composite is clearly illustrated by the scheme shown in Figure 5 on the right, which corresponds, as described above, to the two-stage nature of deformation, while the loading of the sample shows the following sequence:

- from the initial state of the sample length L to the loading corresponding to one of elastic deformation ΔL (Stage 1);
- from the beginning of destruction of the first weft fiber and the matrix to the complete destruction of the entire cross section of the composite sample (Stage 2).

Thus, at the first stage of the loading, the tension of weft fibers, which are involved in the matrix load redistribution within the limits of the elastic deformation, occurs. During the second stage, the exhaustion of some strength weft fibers or groups of fibers occurs. The deformation parameter still does not respond to it, but the intensity of the total AE increment starts to increase. With further loading a sequential load redistribution to the remaining undamaged weft fibers occurs, which leads to a further loss of strength of one or a group of them. The intensity of the total AE increment continues to grow. A further increase in the load apparently causes the process of self-destruction. From this moment, the deformation parameter begins to respond, which, as seen from Figure 4, begins to grow more intensely than the load. There is a rapid increment in both parameters until the complete destruction of the sample cross section occurs. Hence, the beginning of the composite destruction under such a type of load is actually revealed, as seen from the AE data, 5–6% earlier than shown by the deformation parameter. It was confirmed by subsequent tests. The effect of training on the mechanical properties

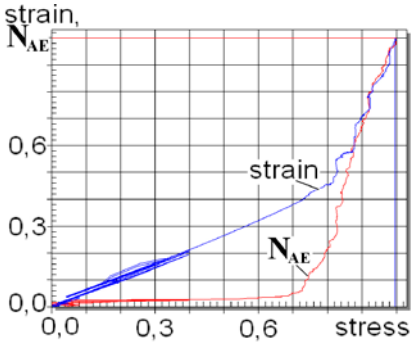

Fig. 6. Dependence of the cumulative AE and the deformation on the stress-strain of a sample with transverse fibers with a triple training corresponding to 40% of the breaking load (sample width: 20 mm)

of test samples with a triple training is characterized by the curve shown in Figure 6.

It is seen that the whole process is similar to the previous test result: there are areas of a proportional change of the deformation parameters and the total AE voltage and the phase of their intensive increment characterizing, similarly to the first case, the beginning of the process of composite irreversible destruction. However, the beginning of the processes of irreversible damage occurs earlier (starting approximately from 0.7 of the rupture stress by the deformation parameter and from 0.65 of the destructive stress by the parameter of the total AE). It can be seen that the training of the sample delayed the beginning of the process of irreversible destruction by approximately 10%.

The results of sample testing with a longitudinal fiber direction along the tensile force are shown in Figure 7, on the right, which presents the graphs of dependence of the deformation and the total AE on the stress in the sample cross section during the static loading. For convenience of analysis and comparative evaluation of test results, the data in the graphs, like in the previous case, is presented in relative units. It can be seen that the whole process of loading in the deformation parameters (see Fig. 7a, curve strain) has almost a linear dependence. However, the nature of the changes in the total AE

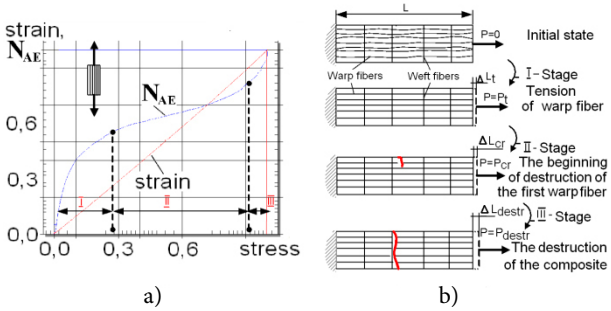

Fig. 7. Graph of the total AE change and the deformation due to the stress-strain (a) and the assumed mechanism for the destruction of the composite in the longitudinal arrangement of base fibers with respect to the tensile force (b)

has a distinctive staging that can be divided into three stages:

- 1st stage – the initial stage of the total AE intensive growth;
- 2nd stage – the stage of the total AE stabilization;
- 3rd stage – the stage of the total AE secondary intensive growth up to the destruction.

All three stages form a single S-shaped curve of the total AE change. Thus, according to the nature of the total AE change, we can evaluate the micro destruction process staging, which cannot be done on the basis of the deformation parameters. Such a nature of the S-shaped behavior of the total AE is observed in all samples with fibers in the longitudinal direction with respect to the applied load.

Figure 8 shows a fragment of the damaged section which was obtained by an electron microscope with a resolution of ×1000. When studying the nature of fiber breakage, it is possible to see the sheaf-shaped placement along the length of the destruction area.

The assumed mechanism of the composite destruction in this case is clearly illustrated by the scheme shown in Figure 7b (right), corresponding to the three-step nature of the deformation, as described above, where the loading of the sample is shown in the following sequence:

- from the initial state of the sample with length L, when the warp fibers are not stretched up to their P_t loading corresponding to their tension before deformation ΔL (Stage 1). An intensive growth of the total AE at this stage is observed mainly due to the micro-cracking of weak spots in the coupling of the matrix with the base fibers;
- from the beginning of the loading, when all the warp fibers are beginning to take the whole load up to the critical load P_{cr} ,when one of the base fibers or a group of fibers is on the verge of losing strength (Stage 2). At this stage the micro-cracking processes occur a little bit slower because they occurred mainly during the first stage, which is reflected in the behavior of the total AE. It becomes more hollow at this stage;

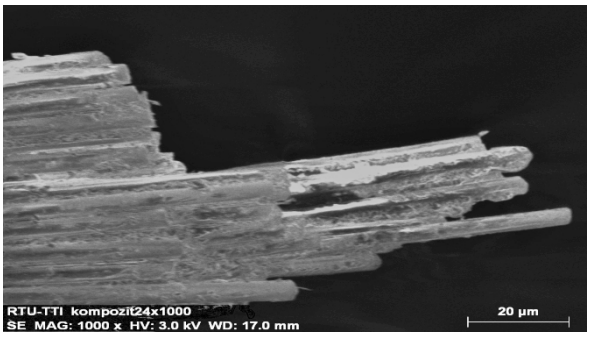

Fig. 8. A fragment of the destroyed portion of the composite (×1000)

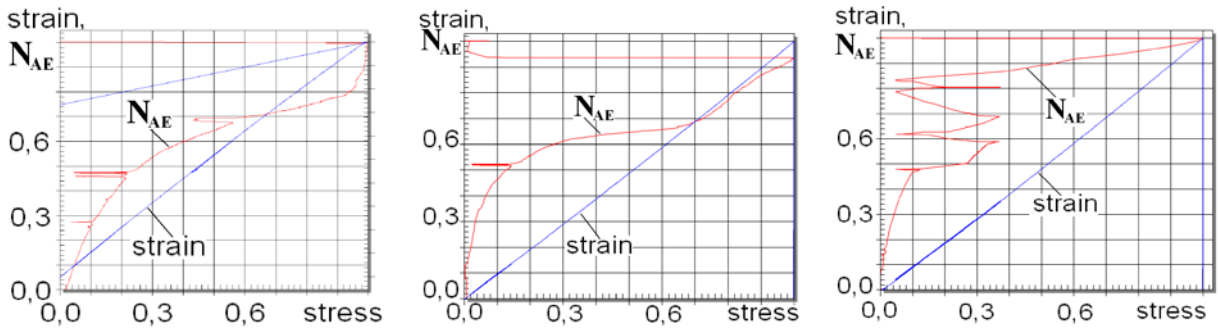

Fig. 9. Dependence of the total AE and the deformation on the stress-strain of a sample with longitudinal fibers: a – with a triple training of 20% of the breaking load (sample width: 20 mm); b – with a six-time training of 15% of the breaking load (sample width: 30 mm); c – with a triple training of 38% of the breaking load (sample width: 30 mm)

– from the beginning of the loading, when one of the base fibers or a group of fibers lose strength up to the loading Pultimate, in which the composite is completely destroyed (Stage 3). At this stage, a sequential redistribution of the load on the remaining intact base fibers occurs in the matrix and a higher load leads to a further loss of strength by another weakest fiber. The intensity of the total AE increment starts to grow. With further loading the process of selfsimilarity of the base fiber destruction occurs, which causes further rapid growth of the total AE. At the same time, the deformation parameter continues to grow uniformly and practically does not respond to any stages of the composite fragmentary strength loss up to its full destruction.

The effect of training equal to 20% of a failure load does not significantly affect the nature of the "S-curvature" of the total AE (Fig. 9a) and, as it can be seen, the "S-curvature" is still present, but both the stage of a stable change of the total AE and the secondary stage of a rapid change in the total AE up to the destruction decrease while the third stage occurs more rapidly than without training.

Further testing of the samples with a training of at least 20% of the ultimate load showed that the S-shaped form remains both with different amounts of training and with the change in the width of the sample, although in these cases the strain measurement, like in the case without training, provides a rectilinear dependence of the deformation on the stress-strain (Fig. 9b). However, the AE shows that the process of a triple training (Fig. 9a) and the process of a six-time training (Fig. 9b) leaves its trace in the form of the Kaiser Effect (Pollock 1989) (horizontal portions of the total AE curve). However, at least a 35% of the breaking load training affects the behavior of the total AE (Fig. 9b). The Kaiser Effect disappears, the process of destruction becomes a two-stage process and the main part of the process occurs at the first stage.

As test results are identical to each other, Figure 10 presents, in relative units, an example of the test results of a sample with the longitudinal fibers along the tensile force as well as the fracture fragments of a sequential destruction of the CFRP under a static loading (Fig. 11).

It is evident that the whole process of damage accumulation according to the AE parameters has a distinct staging that can be split, like in the previous case with fiberglass, into three stages: the initial stage of the total AE intensive growth,

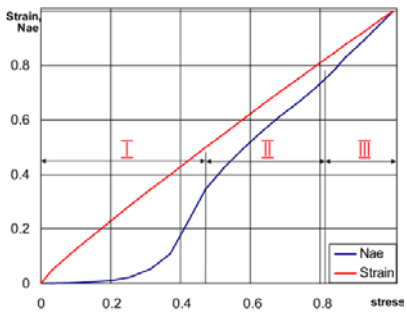

Fig. 10. Graph of the total AE change and the deformation due to the stress-strain with a longitudinal arrangement of warp fibers relative to the tensile force.

Fig. 11. The sequence of the CFRP destruction under a static loading. a – initial state; b – intermediate (the destruction of the matrix); c – final (the destruction of the fibers)

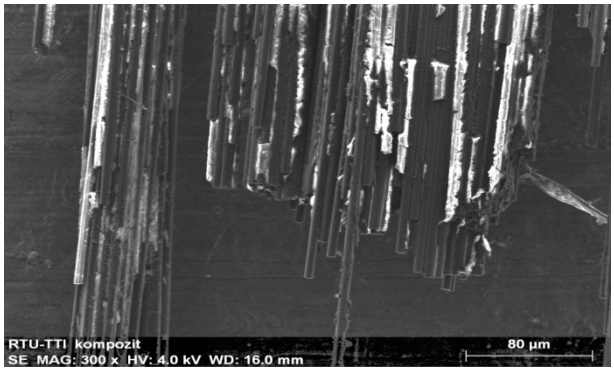

Fig. 12. Photo of the destroyed sample fragment (×300)

the total AE step stabilization and the secondary stage of the total AE intensive growth up to the destruction. However, unlike fiberglass with its "S- shaped" curve, all three stages form a single "bucket" shape of the total AE change. The supposed mechanism of the composite destruction in this case, which is similar to the mechanism of the fiberglass destruction, is illustrated in the scheme shown in Figure 7c, on the right. Figure 12 shows a fragment of the damaged section which was obtained by an electron microscope with a resolution of ×300. When studying the nature of fiber breakage, it is possible to see their sheaf shaped placement along the length of the destruction area, the same as with the sample made of fiberglass (Fig. 6).

Thus, the existing methods for determining the mechanical properties do not allow evaluating the staged process of the destruction of samples with longitudinal fibers with respect to load and take more time to characterize the staging of the destruction process of the samples with the transverse direction of the fibers in relation to the load. Therefore, the use of the AE method for the study of failure micromechanics significantly improves the reliability of the model and accurate methods of determining the mechanical properties of a composite, which is a promising direction of research into the application of the acoustic emission method for determining the mechanical properties of a composite. In addition, further research into the "S-shaped" and "bucket" forms of behavior of the total AE should be directed (with the involvement of fractographic analysis) towards studying the processes in the composite microfracture that are responsible for the formation of such "S-curvatures" and "bucket" shapes of the total AE.

4. Conclusions

For the samples made of fiberglass with transverse fibers with respect to the applied load, the process of destruction both in the deformation parameters and in the parameters of the total AE has two stages of damage accumulation: the stage of proportional changes in these parameters due to stress and the stage of intensive increment of these parameters. At the same time the parameter of the total AE shows that the process of destruction begins 5–6% earlier than it is shown by the deformation parameter.

The nature of the total AE change for the fiberglass and carbon composites with longitudinal fibers with respect to the applied load shows that the process of destruction consists of three stages of damage accumulation that cannot be seen in the parameters of deformation. For the samples made of fiberglass without training or with a training of up to 20% of the ultimate load, the "S-shaped" form of behavior of the total AE is retained in all samples without exception, characterizing a three-stage process of damage accumulation, wherein the triple and six-time training for small values of load (up to 20 % of the failure load) has little influence on the behavior of the total AE curve.

The triple training for large values of load (above 35% of the failure load) exerts a strong influence on the behavior of the total AE curve, and the process of damage accumulation occurs in two-stages.

However, in both the first and the second case the training does not have any influence on the tensile strength at these loading conditions.

Acknowledgements

This work has been supported by the European Regional Development Fund within the project "Development of an experimental long flight distance unmanned aerial vehicle prototype for multi-purpose environmental monitoring (LARIDAE)" No.2DP/2.1.1.1/14/APIA/ VIAA/088.

References

Deniel, I. M. 1978. Fotouprugoe issledovanie kompozitov, v kn. *Mekhanika kompozitsionnykh materialov,* t. 2. M.: Mir, 492–552.

Kelly, A.; Davies, G. J. 1965. The principles of the fibre reinforcement of metal, *Metallurgical Reviews* 10(37): 1–77. https://doi.org/10.1179/mtlr.1965.10.1.1

Korten, G. 1970. Mikromekhanika i kharakter razrusheniya kompozitsiy, v kn. *Sovremennye kompozitsionnye materialy*. M.: Mir, 41–140.

McDanels, D. L.; Jech, R. W.; Weeton, J. W. 1963. *Stress-Strain Behavior of Tungsten-Fiber-Reinforced Copper Composites*, *NASA TN D-1881*. National Aeronautics and Space Administration, Washington, D. C, Oct. 1963

Parratt, N. J. 1960. Defects in glass fibers and their effect on the strength of plastic mouldings, *Rubber and Plastics Age* 41(3): 263–266.

Pollock, A. A. 1989. *Acoustic emission inspection.* Metals handbook, vol. 17. 9th ed. ASM International, Materials Park, Ohio, 278–294.

Pridantsev, S. A. 1978. *Metallicheskie kompozitsionnye materialy*: Ucheb. posobie. Kazan': KAI. 68 s.

Urbach, A.; Banov, M.; Turko, V.; Feshchuk, Y. 2011. Diagnostics of fatigue damage of gas turbine engine blades, *World Academy of Science, Engineering and Technology* 59: 906–911.

Urbahs, A.; Banovs, M.; Turko, V.; Feshchuk, Y. 2012. New approach to use the acoustic emission monitoring for the defects detection of composit-material's design elements, *Ūdens Transports un infrastruktūra: 14 starptautiskā konference*, 26–27 April 2012, Riga, Latvia, 45–50.

Urbahs, A.; Banovs, M.; Turko, V.; Feshchuk, Y.; Khodos, N. 2011. Investigation of micromechanics of plasto-elastic behaviour of anisotropic composite materials under static loading by the acoustic emission method, in *Advances and Trends in Engineering Materials and Their Applications: Conference Proceedings*, 11–15 July 2011, Riga, Latvia.